A Comparison of Algorithms for Subsurface Target Detection and Identification Using Time-Domain Electromagnetic Induction Data

Stacy L. Tantum, *Member, IEEE,* and Leslie M. Collins, *Member, IEEE*

***Abstract*—In this paper, the performance of subsurface target identification algorithms using data from time-domain electromagnetic induction (EMI) sensors is investigated. The response of time-domain EMI sensors to the presence of a conducting object may be modeled as a weighted sum of decaying exponential signals. Although the weights associated with each of the modes are dependent on the target/sensor orientation, the decay rates are a function of the target's composition and geometry and therefore are intrinsic to the target. Since the decay rates are not dependent on target/sensor orientation or other unobservable parameters, decay rate estimation has previously been proposed as a viable method for target identification. The performance attained with Bayesian target identification algorithms operating on the entire time-domain signal and decay rate estimates is compared through both numerical simulations and application to experimental data. The decay rate estimates utilized in the numerical simulations are assumed to achieve the Cramér–Rao lower bound (CRLB), which provides a lower bound on the variance of an unbiased parameter estimate. The simulations as well as results obtained with experimental data show that processing the entire time-domain signal provides better target identification and discrimination performance than processing decay rate estimates.**

***Index Terms*—Bayes procedures, electromagnetic induction (EMI), object detection, parameter estimation, pattern classification.**

I. Introduction

ELECTROMAGNETIC induction (EMI) sensors are one of several sensor modalities employed for subsurface target detection and identification. EMI sensors transmit a primary electromagnetic field that induces currents in any metallic object that the primary field penetrates. When the primary field is abruptly turned off, eddy currents in the metallic object produce a secondary electromagnetic field that is measured by the sensor. The measured EMI response can be modeled as a sum of decaying exponential signals whose characteristic decay rates are intrinsic to the interrogated target. Since the decay rates are not dependent on target/sensor orientation, decay rate estimation has been proposed as an effective and robust method for target identification [1]. Target identification using EMI sensors has been considered previously [2]–[6]. In [2], classification of metal targets using frequency domain EMI sensors is considered, and a Bayesian approach is applied to address the inherent uncertainties concerning the target/sensor orientation. In [3], multifrequency EMI data is utilized for target identification. In [4]–[6], classification of objects using decay rate estimates is investigated.

The optimal algorithm for target identification, in the sense of minimum probability of error, is to choose the target that maximizes the *a posteriori* probability of the hypothesis given the time-domain data. In this paper, the performance of a Bayesian target identification algorithm operating on the decay rate estimates is compared to the optimal algorithm operating on the entire time-domain signal. While processing the entire time-domain signal is optimal, it also may be computationally intensive. One approach that can be taken to reduce the computational intensity is to reduce the dimensionality of the data. Processing a set of parameters derived from the entire signal may also be optimal if those parameters constitute a set of sufficient statistics. Therefore, if the decay rates characterizing the target under consideration form a set of sufficient statistics, the performance will not be degraded by reducing the dimensionality of the data.

The Cramér–Rao lower bound (CRLB) provides a lower bound on the variance of an unbiased parameter estimate. The CRLB is useful in the context of subsurface target identification via decay rate estimation because it provides a means of determining *a priori* how likely it is that targets of interest will be mistaken for each other. It also provides a mechanism for determining how many other objects, presumably clutter, may be mistaken for a particular target of interest and thus contribute to the false alarm rate. In addition, it is a valuable tool in designing systems and/or data collections. With respect to designing systems, the CRLB can be evaluated to determine the number of temporal averages necessary to improve the SNR and reduce the variance on the decay rate estimates to an acceptable level. In the context of data collection, the CRLB can be evaluated to determine *a priori* how taking spatial measurements and measuring a target from several target/sensor orientations will affect performance. In this work, the CRLB is utilized to determine the variance of the decay rate estimates in the simulations. Since the decay rate estimates used in the simulations are the lowest variance unbiased estimates that can be obtained, the performance comparison between processing the entire time-domain signal and the decay rate estimates is not subject to artifacts due to the particular technique chosen for decay rate estimation. Finally, an analysis such as this allows for evaluation of computational complexity in addition to algorithm performance.

Manuscript received June 16, 2000; revised February 28, 2001. This work was supported by SERDP under Grant DACA72-99-C-0012-CU-1123 and JUXOCO under Grant DAAD19-99-1-0201, administered by ARO.

The authors are with the Department of Electrical and Computer Engineering, Duke University, Durham, NC 27708-0291 USA (e-mail: lcollins@ee.duke.edu).

Publisher Item Identifier S 0196-2892(01)04848-3.

The performance comparisons are made using both numerical simulations and data collected at a test site at Fort A.P. Hill, VA, using the U.S. Army's standard issue metal detector. The numerical simulations are performed for a set of four distinct targets. The results show that target identification performance is degraded when the decay rate estimates are processed rather than the entire time-domain signal. At noise levels typical of fielded sensors, these targets are fairly easy to distinguish, however, there is difficulty at higher noise levels (lower SNR). When more targets are present, target identification performance becomes more difficult, and the performance curves will shift toward higher noise variance, and performance will be more like that shown here for simulations at low noise variances. The results obtained with field data from Fort A.P. Hill support the simulation results and demonstrate that the problem becomes more difficult when the number of targets and clutter objects increases.

The remainder of the paper is organized as follows. The signal model is described in Section II. The algorithms for processing the entire signal and the decay rate estimates are discussed in Sections III and IV, respectively. Section V describes the manner in which the probability density functions for the decay rates estimates are determined. The algorithms are applied to simulated data in Section VI, and to data collected at a test site for landmine detection at Fort A. P. Hill in Section VII.

II. Signal Model

Electromagnetic induction (EMI) sensors operate by sensing the radiated field produced by currents induced in a conducting body by a primary field generated by the sensor. Since this phenomenom occurs with any conducting body, an EMI sensor essentially behaves as a metal detector and will measure a response from any body that contains a sufficient quantity of metal such as unexploded ordnance (UXO), landmines, and metallic clutter (i.e., shrapnel).

In order to induce currents that penetrate the conducting body and produce a measurable secondary field, the EMI sensor must operate at sufficiently low frequencies [1]. The displacement current is negligible at the frequencies at which EMI sensors typically operate (< 1 MHz), therefore the measured response of a time-domain EMI sensor may be modeled as weighted sum of decaying exponential signals [7]

$$s(t) = \sum_{i=1}^{N} A_i e^{-\alpha_i t} \tag{1}$$

where α_i is the ith decay rate and A_i is its initial magnitude. Each of the decay rates corresponds to a natural resonant frequency of the interrogated target and is a function of the target's physical attributes, such as its geometry and metal type(s). The amplitudes of each of the exponential decays are related to the target/sensor orientation. Since the decay rates are intrinsic to the target and are not a function of the target/sensor orientation or other unobservable parameters, decay rate estimation has been suggested as an effective method of target identification [1], [5].

The targets of interest in this application (UXO and landmines) have metallic components that are typically cylindrical in shape and therefore may be modeled as bodies of revolution (BOR). A BOR has two principle coordinates, vertical and transverse, and each intrinsic decay rate is associated with one of the two coordinate directions. Time-domain EMI sensors record the late time field which is dominated by the lowest order mode, or slowest decay rate. Thus, the measured response of an EMI sensor may be approximated by a sum of two decaying exponential signals, one in each of the two coordinate directions

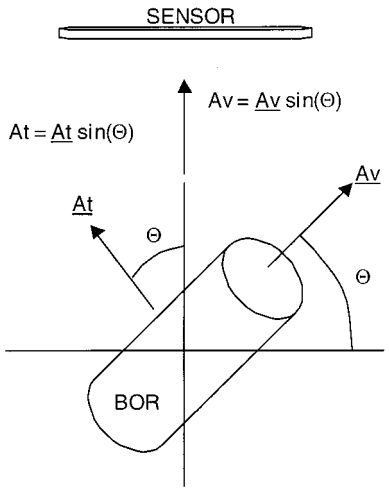

Fig. 1. Typical body of revolution (BOR) and the relationship between the target/sensor orientation and the mode amplitudes.

$$s(t) = A_{\mathrm{v}} e^{-\alpha_{\mathrm{v}} t} + A_{\mathrm{t}} e^{-\alpha_{\mathrm{t}} t} \tag{2}$$

where α_{v} and α_{t} are the decay rates of the vertical and transverse modes, respectively, and A_{v} and A_{t} are their respective amplitudes. The amplitudes associated with each of the decay rates are dependent upon the target/sensor orientation. As the sensor rotates around the BOR, the amplitudes vary sinusoidally and each mode is maximally excited when the sensor is located along the axis corresponding to that mode. In theory, when the sensor is oriented along the vertical axis only the vertical mode is excited, thus $A_{\mathrm{v}} = \underline{A_{\mathrm{v}}}$ and $A_{\mathrm{t}} = 0$. Similarly, when the sensor is oriented along the transverse axis, only the transverse mode is excited, thus $A_{\mathrm{v}} = 0$ and $A_{\mathrm{t}} = \underline{A_{\mathrm{t}}}$. A typical BOR and the relationship between the target/sensor orientation and the mode amplitudes are illustrated in Fig. 1.

III. Target Identification Using the Entire Signal

Target identification may be viewed as a multiple hypothesis problem, in which each of the N targets of interest corresponds to a hypothesis. When this problem is approached using Bayesian principles, the goal is to develop a decision rule which minimizes the average cost of making a decision. If we assume the cost associated with any incorrect decision is 1 and the cost associated with a correct decision is 0, the Bayes decision rule is to choose the hypothesis which maximizes the *a posteriori* probability of the hypothesis given the measurement $\mathbf{r}$ [8], [9]

$$f(H_i|\mathbf{r}) = \frac{f(\mathbf{r}|H_i) f(H_i)}{f(\mathbf{r})} \tag{3}$$

where

$f(\mathbf{r}|H_i)$ distribution of the data given the hypothesis;
$f(H_i)$ prior distribution on the hypotheses;
$f(\mathbf{r})$ probability of the measurement.

Since $f(\mathbf{r})$ is independent of the hypotheses, the decision rule reduces to choosing the hypothesis H_i, which maximizes $f(\mathbf{r}|H_i)f(H_i)$. If all of the hypotheses are equally likely *a priori* (i.e., $f(H_i) = (1/N)\ \forall i$), then the decision rule further reduces to choosing the hypothesis that maximizes $f(\mathbf{r}|H_i)$, which is the likelihood of the measurement under hypothesis H_i. This is the decision rule for maximum likelihood (ML) decision criteria. Thus, under the assumption of uniform prior probabilities for the hypotheses, the maximum likelihood and Bayesian decision rules are equivalent, and the hypothesis H_i is chosen according to

$$\max_{H_i} \{f(\mathbf{r}|H_i)\}, \qquad i = 1, 2, \ldots, N. \tag{4}$$

The above Bayesian decision rule implicitly assumes all the parameters defining the signal associated with each hypothesis are known with complete certainty. However, in many applications of practical interest, there is often uncertainty regarding the signals. In the context of subsurface target identification using time-domain EMI data, the amplitudes of the decay rates A_{v} and A_{t} are not known *a priori* because they are dependent on the target/sensor orientation, which is unknown since the target is buried. Thus, even though the decay rates of each of the targets of interest are known *a priori*, the amplitudes of the decay rates are not known and as a result there is some uncertainty regarding the measured signal for each of the targets of interest. The uncertainty concerning the measured signal can be accounted for within a Bayesian framework by integrating over the uncertain parameters to calculate the likelihood of the measurement under each hypothesis before applying the decision rule (4)

$$f(\mathbf{r}|H_i) = \int_A f(\mathbf{r}|H_i, \boldsymbol{A}) f(\boldsymbol{A}|H_i) f(\boldsymbol{A})\, d\boldsymbol{A} \tag{5}$$

where $\boldsymbol{A} = \{A_{\mathrm{v}}, A_{\mathrm{t}}\}$ is a vector consisting of the amplitudes of each of the decay rates. The integration in (5) can be computationally intensive, so Monte Carlo integration techniques are often employed [10]. An alternative approach is to first estimate the amplitudes, and then use those estimates, $\hat{\boldsymbol{A}}$, as though they are known parameters to approximate (4) as

$$f(\mathbf{r}|H_i) \approx f(\mathbf{r}|H_i, \hat{\boldsymbol{A}}). \tag{6}$$

This suboptimal approach is similar to a generalized likelihood ratio test (GRLT) and performance may be degraded from an optimal method, but it has the benefit of greatly reduced computational complexity.

The time-domain response of EMI sensors is typically recorded at K discrete sample times. Therefore, the measured response, $\mathbf{r}$, is a $K \times 1$ vector containing the sampled signal $\mathbf{s}$ and measurement noise $\mathbf{n}$

$$\mathbf{r} = \mathbf{s} + \mathbf{n}. \tag{7}$$

The noise corrupting the EMI measurement $\mathbf{n}$ is assumed to be independent identically distributed (i.i.d.) Gaussian noise with variance σ_n^2. Under this assumption, the *a posteriori* probability of the measurement under hypothesis H_i given the decay rate amplitudes is

$$f(\mathbf{r}|H_i, \boldsymbol{A}) = \frac{1}{(2\pi\sigma_n^2)^{K/2}} \cdot \exp\left\{-\frac{1}{2\sigma_n^2}(\mathbf{r} - \mathbf{s}_i(\boldsymbol{A}))^T(\mathbf{r} - \mathbf{s}_i(\boldsymbol{A}))\right\} \tag{8}$$

where $\mathbf{s}_i(\boldsymbol{A})$ is the signal corresponding to target i with decay rate amplitudes $\boldsymbol{A}$. This relationship is utilized in (5) to calculate the decision metric for each target of interest.

IV. Target Identification Using Decay Rate Estimates

Under the assumed signal model for a BOR (2), each target possesses a unique set of decay rates, $\boldsymbol{\alpha} = \{\alpha_{\mathrm{v}}, \alpha_{\mathrm{t}}\}$. Therefore, if the intrinsic decay rates can be accurately and reliably estimated from the measured sensor response, the interrogated target can be identified. The Bayesian decision rule for this approach is the same as for when the entire time-domain signal is utilized (4). In this case, the measurement $\mathbf{r}$ consists of the estimated decay rate(s) rather than the sampled signal. In this formulation, the Gaussian noise process is assumed to be independent between samples, but not identically distributed because the variance of each decay rate estimate is different. Under these assumptions, the *a posteriori* probability of the measurement under hypothesis H_i is

$$f(\mathbf{r}|H_i) = \frac{1}{(2\pi)^{K/2}|\boldsymbol{\Sigma}|^{1/2}} \cdot \exp\left\{-\frac{1}{2}(\mathbf{r} - \boldsymbol{\alpha}_i)^T\boldsymbol{\Sigma}^{-1}(\mathbf{r} - \boldsymbol{\alpha}_i)\right\} \tag{9}$$

where $\boldsymbol{\alpha}_i$ contains the decay rate(s) for target i, and $\boldsymbol{\Sigma}$ is the covariance matrix of $\mathbf{r}$. The decay rate estimates are assumed to be unbiased, uncorrelated Gaussian random variables. Thus, $\boldsymbol{\Sigma}$ is a diagonal matrix containing the variances of each of the decay rate estimates, where the jth diagonal element of $\boldsymbol{\Sigma}$ is $\sigma_{\alpha_j}^2$, and j is the index on the decay rates characterizing the signal.

V. Decay Rate Estimation

The performance attained by target identification algorithms that utilize decay rate estimates is directly related to the accuracy of those estimates. The CRLB provides the lower bound on the variance of an unbiased parameter estimate. For the purposes of the numerical simulations in the following section, the decay rate estimates are assumed to be unbiased Gaussian random variables whose variance achieves the CRLB. Decay rate estimates that achieve the CRLB are the best (i.e., lowest variance) unbiased estimates attainable and therefore will provide an upper bound on target identification performance using decay rate estimates.

The CRLBs for poles and amplitude coefficients for damped exponential signals have been previously derived under the as-

sumption that the signal is linearly sampled starting at time $t = 0$ [11]. The poles p_i considered in the derivation of the CRLBs are related to the decay rates α_i considered in this work by $p_i = e^{\alpha_i T}$, where T is the sampling interval. In practice, the assumption that the initial sample time is at $t = 0$ is not valid for pulsed EMI systems because it is not possible to begin recording the response until some time after $t = 0$ in order to avoid interference from the incident pulse. The CRLBs for pole and amplitude coefficient estimates have been generalized to accommodate arbitrary temporal sampling with any initial sample time [12]. However, for simplicity this issue is not considered in these simulations.

The CRLBs provide the lower bound on the variance of the pole estimates for a fixed set of poles with a fixed set of amplitudes. However, in this application the amplitudes of the poles are not known *a priori*. The unconditional distribution of the pole estimate is

$$f(p_i) = \int_A f(p_i|\boldsymbol{A}) f(\boldsymbol{A})\, d\boldsymbol{A}. \tag{10}$$

Assuming that given the pole amplitude the pole estimate is unbiased and follows a Gaussian distribution with variance given by the CRLB $\sigma_p^2(\boldsymbol{A})$, the distribution in (10) is also an unbiased Gaussian distribution and its variance is given by

$$\sigma_p^2 = \int_A \sigma_p^2(\boldsymbol{A}) f(\boldsymbol{A})\, d\boldsymbol{A} = \mathcal{E}\{\sigma_p^2(\boldsymbol{A})\} \tag{11}$$

where $\mathcal{E}\{\cdot\}$ is the expectation operator. This is the Gaussian distribution used for the pole estimates in the numerical simulations.

Since the decay rate, rather than the pole, is the parameter of interest, the variance of the decay rate estimate is derived from the variance of the pole estimate. The pole estimate, $\hat{p}_i$, can be transformed to a decay rate estimate, $\hat{\alpha}_i$, by

$$\hat{\alpha}_i = g(\hat{p}_i) = \frac{-\ln \hat{p}_i}{T}. \tag{12}$$

The variance of the decay rate estimate may be calculated from the CRLB for the variance of the pole estimate by

$$\begin{aligned} \mathrm{Var}\{\hat{\alpha}_i\} &= \mathrm{Var}\left\{\frac{-\ln \hat{p}_i}{T}\right\} \\ &= \mathcal{E}\left\{\left(\frac{-\ln \hat{p}_i}{T}\right)^2\right\} - \left(\mathcal{E}\left\{\frac{-\ln \hat{p}_i}{T}\right\}\right)^2. \end{aligned} \tag{13}$$

The expectation integrals are evaluated numerically to determine the variances of the decay rate estimates. The CRLB indicates that the variance of the decay rate estimates is a function of both the number of decay rates estimated and the relative amplitudes of the decay rates. In general, more decay rates will increase the variance of the estimates and lower amplitudes will increase the variance of the estimates [11].

VI. Numerical Simulations

Target identification performance is first evaluated and compared through numerical simulations. Results attained with data collected at a test site at Fort A.P. Hill are presented in the following section [Section VII]. Four synthetic targets considered for the simulations, and their intrinsic decay rates are listed in Table I. The four time-domain signals are generated according to (2) and sampled from 0 to 0.75 ms at a sampling frequency of 2 MHz. The maximum amplitudes of each of the modes, $\underline{A_{\mathrm{v}}}$ and $\underline{A_{\mathrm{t}}}$, are set equal to 1. Example signals for each target are shown in Fig. 2 for $A_{\mathrm{v}} = A_{\mathrm{t}} = 0.5$. All of the simulation results presented in the section were generated from 2250 independent Monte Carlo iterations. *A priori*, the angle Θ between the target and sensor is assumed to follow a uniform distribution, and the prior distribution on the target is also assumed to be uniform.

TABLE I
Simulated Target Vertical (α_{v}) and Transverse (α_{t}) Decay Rates

Target	α_{v}	α_{t}
1	10000	14000
2	16000	22000
3	25000	35000
4	32000	45000

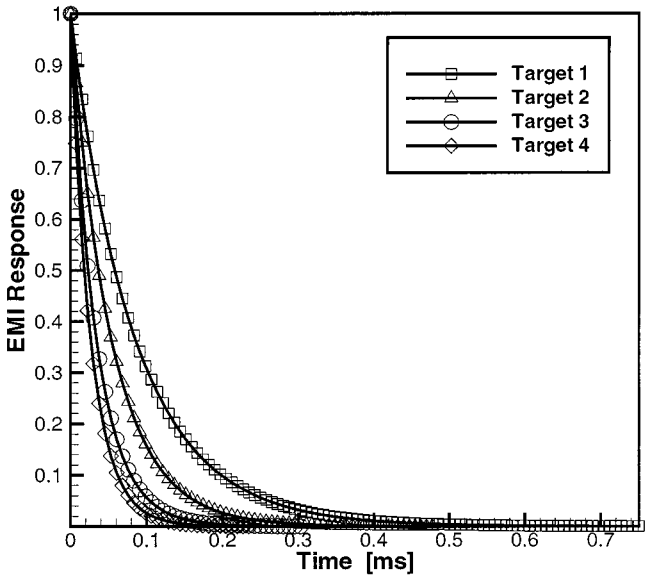

Fig. 2. Noise free time-domain signals for the four simulated targets with $A_{\mathrm{v}} = A_{\mathrm{t}} = 0.5$.

The target identification performance results are presented as a function of the noise variance. The noise variance is related to the SNR by $\mathrm{SNR} = E_s/\sigma_n^2$, where E_s is the signal energy. The signal energy, and therefore the SNR, for each signal is dependent upon the decay rates and the decay rate amplitudes. For this particular set of simulated targets with this set of sampling parameters, the range of SNRs associated with a particular noise level is related to the noise variance by

$$\mathrm{SNR\ [dB]} \approx 10(k+1) \text{ to } 10(k+2)\ \mathrm{dB} \tag{14}$$

where the noise variance is 10^{-k}. For example, when the noise variance is 10^{-4} the SNR for the measured time-domain signal ranges from 50 to 60 dB. The magnitude of the noise when $\sigma_n^2 = 10^{-4}$ is illustrated in Fig. 3, again for $A_{\mathrm{v}} = A_{\mathrm{t}} = 0.5$.

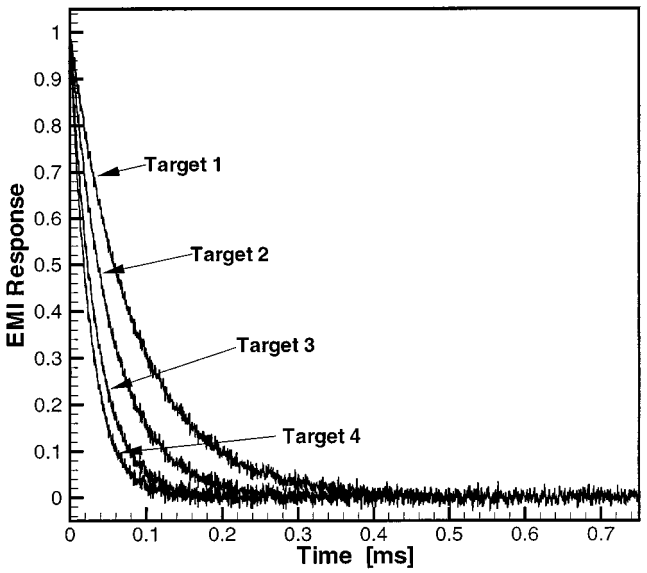

Fig. 3. Noisy time-domain signals for the four simulated targets with $A_{\mathrm{v}} = A_{\mathrm{t}} = 0.5$ and $\sigma_n^2 = 10^{-4}$ (SNR = 50 to 60 dB).

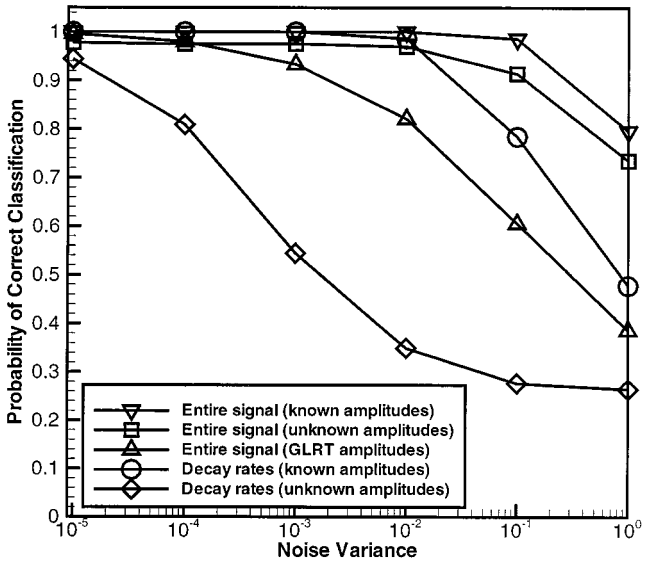

Fig. 4. Probability of correct classification ($\mathrm{P_{CC}}$) as a function of noise variance for algorithms operating on the entire signal and the estimated decay rates.

When considering performance attained by algorithms operating on decay rate estimates, it is assumed the decay rate estimates achieve the CRLB. The CRLB defines the lowest variance of unbiased decay rate estimates, and therefore performance evaluated under this assumption provides an upper bound on target identification performance achievable using decay rate estimates. Decay rate estimation algorithms that do not achieve the CRLB will not perform better than the results presented here.

The average probability of correctly stating which of the four known targets is present is shown in Fig. 4 as a function of the noise variance for algorithms utilizing the entire signal (4)–(6) and decay rate estimates (9). As expected, the probability of correctly identifying the target increases as the noise variance decreases. The scenario in which the amplitudes of the decay rates are known *a priori* provides an upper bound on target identification performance. This situation is artificial, in that the decay rate amplitudes are rarely, if ever, known *a priori* in the context of subsurface target identification. However, since the only unknown parameters are the decay rates, which are the defining parameters for the targets, this scenario does provide an upper bound on performance, against which the performance attained when the amplitudes are unknown can be compared, and the loss in performance due to the uncertainty in the decay rate amplitudes quantified. Since these results were obtained through simulation, the signal model describing the simulated data is complete, meaning there are no factors unaccounted for in the model. Therefore, the effects of uncertainty regarding the defining parameters, the decay rates and their amplitudes in this case can be isolated.

The situation in which the decay rate amplitudes are not known *a priori* is most representative of the problem encountered in subsurface target identification. When processing either the entire signal or decay rate estimates, performance is degraded from the level attained when the amplitudes are known *a priori*. If the noise level is low enough (less than 10^{-4} in this example), then the decay rate amplitudes can be readily and accurately estimated by a least squares approach. In this case, performance approaches that achieved when the amplitudes are known *a priori* by implementing a GLRT-like identification algorithm which operates on the entire signal. However, if the noise level exceeds the threshold at which the amplitudes can be reliably estimated, then the performance attained by this algorithm is substantially lower than that attained by an algorithm which operates on the entire signal and integrates over the inherent uncertainty in the decay rate amplitudes. This effect is illustrated in Fig. 4. Regardless of whether or not the decay rate amplitudes are known *a priori*, the algorithms operating on the decay rate estimates do not perform as well as algorithms operating on the entire time-domain signal which assume the same level of *a priori* knowledge. Processing any set of sufficient statistics derived from the original time domain signal would provide the same level of performance as processing the original signal. Since the decay rate estimates achieve the CRLB and thus are the lowest variance unbiased estimates that can be obtained, the degradation in performance can be attributed to the fact that the decay rates do not constitute a set of sufficient statistics.

When the number of targets of interest is increased, the performance curves shift toward higher noise variance (lower SNR). Thus, in order to maintain a particular level of performance with a larger set of targets, the noise variance must be decreased. Similarly, when the number of targets is small, the tolerance for noise is greater.

Confusion matrices for each of the target identification algorithms are presented in Tables II–IV for a noise variance of $\sigma_n^2 = 10^{-4}$. At this noise level, target identification with known decay rate amplitudes is perfect, so those confusion matrices are not shown. The confusion matrices tabulate the probability that a given target is identified as a particular target and illustrate the degree to which two targets are mistaken for one another. The diagonal of these matrices are the probabilities the

TABLE II
CONFUSION MATRIX FOR PROCESSING THE ENTIRE TIME-DOMAIN SIGNAL WITH UNKNOWN DECAY RATE AMPLITUDES ($\sigma_n^2 = 10^{-4}$)

True Target \ Classified Target	T1	T2	T3	T4
T1	1	0	0	0
T2	0	1	0	0
T3	0	0	0.93	0.07
T4	0	0	0.03	0.97

TABLE III
CONFUSION MATRIX FOR PROCESSING THE ENTIRE TIME-DOMAIN SIGNAL WITH GLRT DECAY RATE AMPLITUDES ($\sigma_n^2 = 10^{-4}$)

True Target \ Classified Target	T1	T2	T3	T4
T1	1	0	0	0
T2	0	1	0	0
T3	0	0	0.96	0.04
T4	0	0	0.04	0.96

TABLE IV
CONFUSION MATRIX FOR PROCESSING THE DECAY RATE ESTIMATES WITH UNKNOWN DECAY RATE AMPLITUDES ($\sigma_n^2 = 10^{-4}$)

True Target \ Classified Target	T1	T2	T3	T4
T1	0.95	0.03	0.01	0.01
T2	0.11	0.82	0.04	0.02
T3	0.05	0.09	0.70	0.17
T4	0.04	0.02	0.17	0.77

targets are correctly identified. At this noise variance, targets 1 and 2 are always correctly identified when the entire signal is processed and the only confusion occurs between targets 3 and 4. However, when the decay rate estimates are utilized for target identification, this is no longer true. The probability of correctly identifying every target is lower when compared to performance achieved processing the entire signal, and each target is confused with all the other targets. Also, note that processing the entire signal under the assumption that the decay rate amplitudes are accurate provides better classification performance for target 3 than integrating over the uncertainty concerning the decay rate amplitudes. However, the opposite is true for target 4. This illustrates the sensitivity of the GLRT-like processor to the accuracy of the decay rate amplitude estimates. In general, targets are more likely to be confused when their characteristic decay rates are more similar.

The improved performance attained by processing the entire time domain signal is achieved at the expense of increased computational intensity. The time required to process the entire signal when the decay rate amplitudes are unknown (the Bayesian processor) is about 1.6 times that required to process the decay rates. The time required to process the entire signal when the decay rate amplitudes are unknown and are estimated (the GLRT-like processor) is about 1.1 times that required to process the decay rates. This is a modest increase in computation time to achieve a significant increase in classification performance. However, these comparisons do not include the time necessary to estimate the decay rates before they are processed. If that step were included, the differences in time requirements would be less and processing the entire signal would compare more favorably to processing the decay rates.

VII. RESULTS WITH JUXOCO TEST SITE DATA

The simulation study suggests that if the goal is to achieve the highest level of performance, the entire time-domain signal should be processed rather than the estimated decay rates. In order to validate these results, processors operating on estimated decay rates and the entire time-domain signal are applied to real data collected with a modified version of the U.S. Army's currently fielded metal detector.

The Joint UXO Coordination Office (JUXOCO) at Ft. Belvoir, VA, is sponsoring a series of experiments designed to establish a performance baseline for a variety of sensors [13]. This baseline will be used to measure the potential improvements in performance offered by advanced signal processing algorithms. In conjunction with this effort, data from low-metal content mines has been gathered using a variety of sensors. Algorithms operating on the entire time-domain response and decay rate estimates have been developed for a modified version of the standard Army metal detection sensor, the PSS-12. These algorithms are applied to data collected at the JUXOCO test site at Fort A. P. Hill, in order to evaluate the their discrimination performance. In the remainder of this section, the sensor, the data collection site and mechanisms, the various algorithms and their performance are discussed.

A. PSS-12 Sensor Description

Schiebel Corporation of Austria manufactures the U.S. Army's currently fielded metal detector, which the U.S. Army designates the AN/PSS-12. The PSS-12 is a pulsed induction device. Its search head uses two concentric coils. The outer is used for transmit and the inner for receive. In the fielded version of the PSS-12, internal circuitry controls the transmit pulse and gates the received signal. The received signal is sampled after decaying from its saturated value for a fixed amount of time, and then an estimated background signal is subtracted from this value. After comparison to a threshold set by the user, this signal drives a voltage to frequency converter to generate an audible tone. The user then interprets the tone to determine the presence of an object. For the JUXOCO site data collection, the PSS-12 was modified so that the entire signal obtained at the

receive coil, or time-decay curve can be measured [14]. This time-domain response is captured electronically via custom designed software written in Labview, which allows the user to control the sampling rate and triggering characteristics. The signal is measured directly from the receive coil of the PSS-12. None of the post-processing performed by the Schiebel electronics has been applied to this signal.

B. Data Collection

Fort A.P. Hill was selected as the location for the JUXOCO test site. The 50 m $\times$ 20 m blind test grid and the 5 m $\times$ 25 m calibration area are sectioned into 1 m $\times$ 1 m squares. Each square has either nothing, a piece of clutter, or a landmine buried at the center. Initially, the site was cleared and all indigenous clutter was removed. The indigenous clutter included rusted shrapnel, expended 0.50 and 0.30 caliber cases, rusted nails, pieces of wire, small copper pieces, and other unidentifiable metal. Samples of the clutter were emplaced in the grid squares to provide discrete opportunities for false alarms. Mine targets emplaced in the grid squares were predominately low-metal content mines since these are the most challenging to detect using EMI sensors. Approximately 100 mines were buried in the blind test grid at tactical depths. At least one mine of each type placed in the calibration grid and representative samples of clutter were also buried in the calibration area. The ground truth associated with the calibration area is available; however, the ground truth associated with the main, or blind, test grid is sequestered. Algorithm developers provide the output of their algorithms for each grid square, or decision opportunity, to JUXOCO for scoring, thus simplifying the calculation of the detection and false alarm probabilities. Further details regarding the data collection plan can be found in [13].

Data was collected from the PSS-12 receive coil in late February of 2000 at the JUXOCO test site by researchers from Auburn University, Auburn, AL. Data was collected three times in the calibration grid and once in the blind grid. During each collection, receive-coil data was measured at the center of each grid square. The signal measured from the receive coil was sampled at 20 MHz and written to an ASCII file. No background signature was subtracted from the measured signals, as background was not tracked for this data collection.

C. Signal Processing and Results

Two algorithm approaches which parallel those described in the simulation study were pursued for the PSS-12 receive-coil data to discriminate between landmines and clutter/blanks. One method first estimated a decay rate from the measured data, and then used the decay rates for target discrimination. The second method used the measured signal in its entirety for target discrimination.

In the first approach, a nonlinear least squares estimation procedure was utilized to estimate a single decay rate associated with each measurement and a GLRT was applied to the estimated decay rates. The probability density functions which described the decay rate data under the two hypotheses were estimated using the calibration lane data, then a GLRT was applied using

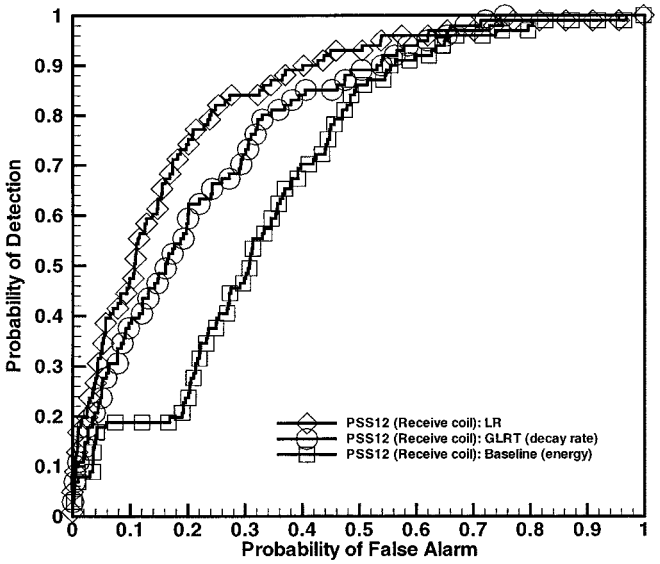

Fig. 5. Comparison of algorithms operating on the entire signal (LR) and the estimated decay rates (GLRT) for the PSS12 receive coil data collected at the JUXOCO test site.

$$\text{GLRT(square)} = \frac{f(\mathbf{r}|H_1)}{f(\mathbf{r}|H_0)} \tag{15}$$

where $f(\mathbf{r}|H_1)$ is the distribution of the decay rates under H_1 (landmine), and $f(\mathbf{r}|H_0)$ is the distribution of the decay rates under H_0 (clutter/blank). The probability density functions (pdfs) were modeled using Gaussian mixture densities.

The second approach utilized the entire signal in a likelihood ratio framework. It was assumed that if the decay rate for a particular object was known, then the pdf for the measured data would be given by

$$f(\mathbf{r}|\alpha, H_i) = N(e^{-\alpha \underline{t}}, \sigma_n^2 I) \tag{16}$$

where $\underline{t}$ is a vector of sample times. However, since the decay rate is not known *a priori*, the likelihood ratio formulation is given by

$$\text{LR(square)} = \frac{\displaystyle\int_\alpha f(\mathbf{r}|\alpha, H_1) f(\alpha|H_1)\, d\alpha}{\displaystyle\int_\alpha f(\mathbf{r}|\alpha, H_0) f(\alpha|H_0)\, d\alpha}. \tag{17}$$

The integration over the uncertainty in the characteristic decay rates was carried out via Monte Carlo methods [10].

The performance of these two approaches on the PSS-12 receive-coil data is shown in Fig. 5. The baseline performance of a standard energy detector is also shown for comparison. These results illustrate the improvement in performance realized by processing the entire signal over processing the estimated decay rates. However, the performance gains are achieved at the cost of increased computational complexity.

VIII. Conclusion

In this paper, target identification performance achieved by processing the entire time-domain signal and the estimated decay rates is compared through numerical simulations and processing real data collected at the JUXOCO test site at Fort A. P. Hill. Numerical simulations are performed assuming there are four targets of interest, each with a distinct set of two characteristic decay rates. The entire time-domain signal and the decay rate estimates are each processed within a Bayesian context, and the optimal processors are implemented. The simulation results show that processing the entire signal provides better target identification performance than processing the decay rate estimates.

The decay rate estimates utilized in the simulations are assumed to achieve the CRLB, and thus are the lowest variance unbiased estimates one can obtain. If the decay rates constitute a set of sufficient statistics then they contain all the information conveyed by the time-domain signal, and optimally processing the decay rates will provide the same level of performance as optimally processing the entire signal. Since the optimal processors were applied to both the time-domain signal and the decay rate estimates and processing the entire time-domain signal consistently provides better target identification performance than processing the decay rate estimates, the degradation in performance resulting from processing only the decay rate estimates can be attributed to the fact that the decay rates do not constitute a set of sufficient statistics and information is lost in representing the response with the decay rate estimates.

The simulation results suggest that if the goal is to achieve the highest level of performance, the entire time-domain signal should be processed rather than the estimated decay rates. The simulation results also illustrate how the CRLB for decay rate estimates may be applied to evaluate system performance. The degree of confusion between targets of interest can be evaluated, and the potential for clutter objects to be incorrectly identified as a target of interest can also be investigated. Results attained by processing data collected at the JUXOCO test site at Fort A.P. Hill illustrate the improvement in discrimination performance realized by processing the entire time-domain signal rather than the estimated decay rates, and support the simulation results.

Acknowledgment

The authors would like to thank Dr. L. Carin for his assistance with the phenomenological model, Dr. L. Riggs and his colleagues at Auburn University, Auburn, AL, for providing access to the data collected at the JUXOCO test site, and Dr. D. Weaver and his colleagues at JUXOCO for scoring the algorithms.

References

[1] C. E. Baum, Ed., *Detection and Identification of Visually Obscured Targets*. Philadelphia, PA: Taylor & Francis, 1999.

[2] P. Gao, L. M. Collins, P. Garber, N. Geng, and L. Carin, "Classification of landmine-like metal targets using wideband electromagnetic induction," *IEEE Trans. Geosci. Remote Sensing*, vol. 38, pp. 1352–1361, May 2000.

[3] D. Keiswetter, I. J. Won, B. Barrow, and T. Bell, "Object identification using multifrequency EMI data," in *UXO Forum '99*, Atlanta, GA, May 1999.

[4] L. S. Riggs, J. E. Mooney, and D. E. Lawrence, "Identification of metallic mine-like objects using low frequency magnetic fields," *IEEE Trans. Geosci. Remote Sensing*, vol. 39, pp. 56–66, Jan. 2001.

[5] G. D. Sower and S. P. Cave, "Detection and identification of mines from natural magnetic and electromagnetic resonances," in *Proc. SPIE*, Orlando, FL, Apr. 1995.

[6] A. H. Trang, P. V. Czipott, and D. A. Waldron, "Characterization of small metallic objects and nonmetallic anti-personnel mines," in *Proc. SPIE*, Orlando, FL, April 1997.

[7] P. Gao and L. M. Collins, "A theoretical performance analysis and simulation of time-domain EMI sensor data for land mine detection," *IEEE Trans. Geosci. Remote Sensing*, vol. 38, pp. 2042–2055, July 2000.

[8] R. N. McDonough and A. D. Whalen, *Detection of Signals in Noise*, 2nd ed. San Diego, CA: Academic, 1995.

[9] H. L. Van Trees, *Detection, Estimation, and Modulation Theory, Pt. I*. New York: Wiley, 1968.

[10] W. H. Press, S. A. Teukolsky, W. T. Vetterling, and B. P. Flannery, *Numerical Recipes in C: The Art of Scientific Computing*, 2nd ed. New York: Cambridge Univ. Press, 1992.

[11] W. M. Steedly and R. L. Moses, "The Cramér–Rao lower bound for pole and amplitude coefficient estimates of damped exponential signals in noise," *IEEE Trans. Signal Processing*, vol. 41, pp. 1305–1318, Mar. 1993.

[12] S. L. Tantum and L. M. Collins, "Physics-based statistical signal processing for improved landmine detection and classification via decay rate estimation," in *Proc. SPIE*, vol. 4038, Orlando, FL, April 2000.

[13] "Hand held metallic mine detector performance baselining collection plan," Tech. Rep., JUXOCO, Ft. Belvoir, VA.

[14] L. Riggs, "Operating characteristics of the AN-PSS12," Tech. Rep., JUXOCO, Ft. Belvoir, VA, 1999.

Stacy L. Tantum (S'92–M'99) was born in 1972 in Trenton, NJ. She received the B.S.E.E. degree in electrical engineering and economics from Tufts University, Medford, MA, in 1994, and the M.S. and Ph.D. degrees in electrical engineering, both from Duke University, Durham, NC, in 1996 and 1998, respectively.

She was a Summer Research Assistant with SACLANT Undersea Research Center, La Spezia, Italy, in 1996. Since 1999, she has been an Assistant Research Professor with the Electrical and Computer Engineering Department, Duke University, Durham, NC. Her current research interests include statistical signal processing with application to remote sensing and ocean acoustics.

Dr. Tantum is a member of Tau Beta Pi, Eta Kappa Nu, and Sigma Xi.

Leslie M. Collins (M'96) was born in 1963 in Raleigh, NC. She received the B.S.E.E. degree from the University of Kentucky, Lexington, in 1985, and the M.S.E.E. and Ph.D. degrees in electrical engineering, both from the University of Michigan, Ann Arbor, in 1986 and 1995, respectively.

She was a Senior Engineer with the Westinghouse Research and Development Center, Pittsburgh, PA, from 1986 to 1990. In 1995, she became an Assistant Professor in the Electrical and Computer Engineering Department, Duke University, Durham, NC. Her current research interests include incorporating physics-based models into statistical signal processing algorithms, and she is pursuing applications in subsurface sensing as well as enhancing speech understanding by hearing impaired individuals.

Dr. Collins is a member of Tau Beta Pi, Eta Kappa Nu, and Sigma Xi.